



CrossMark  
click for updates

Cite this: *Soft Matter*, 2016,  
12, 4214

## Ant aggregations self-heal to compensate for the Ringelmann effect†

Sulisay Phonekeo,<sup>a</sup> Tanvi Dave,<sup>a</sup> Matthew Kern,<sup>b</sup> Scott V. Franklin<sup>b</sup> and David L. Hu<sup>\*ac</sup>

Fire ants, *Solenopsis invicta*, link their bodies together to form structures such as rafts, bivouacs and bridges. Such structures are in danger of being damaged by natural disturbances such as passing water currents. In this combined experimental and theoretical study, we investigate the self-healing of ant assemblages. We press two ant aggregations together and measure the forces to pull them apart. As the group size increases, the contribution of each ant decreases. This phenomenon, known as the Ringelmann effect, or social loafing, has previously been shown for cattle and humans. In this study, we show that it is a challenge for ants as well. We rationalize this effect with an agent-based simulation which exhibits the Ringelmann effect of ants that periodically make and break links with each other, but grip with higher probability if the ants are stretched. Over time, ants compensate for the Ringelmann effect by building more links. We use a mathematical model to show that the rate of new links is proportional to the number of free ants in the cluster. The principles found here may inspire new directions in self-healing and active materials.

Received 11th January 2016,  
Accepted 15th March 2016

DOI: 10.1039/c6sm00063k

[www.rsc.org/softmatter](http://www.rsc.org/softmatter)

## 1 Introduction

The ability to repair oneself is a hallmark of all life. Designing systems to self-repair is one of the dreams of engineering, as it would increase the lifetime and autonomy of our devices. Over the years, a number of designs have been proposed. Devices that mimic blood flow and clotting have been developed. Self-healing polymers can use chemical reactions to heal, and can even regain up to 97 percent of their original tensile strength.<sup>1</sup> Nearly all human-made self-healing methods rely upon extrusion of fluid or chemical bonding. In this study, we consider ants, which exhibit a type of macroscopic self-healing that is more similar to how multicellular and swarm organisms heal.

Natural self-healing occurs whenever we cut ourselves. The scab formation process involves the migration of cells on the short time-scale and regeneration of cells on the long-time scale. Both are stimulated through chemical signaling pathways.<sup>2</sup> This migration and growth is responsible for the closing and healing of skin wounds.<sup>3,4</sup> Self-healing occurs on the larger scale as well. Swarms of organisms such as a flock of birds reorganizes itself after the attack of a predator. This reorganization of individuals can also be seen as a kind of self-healing.

Fire ants represent a new model system to investigate self-healing.<sup>5</sup> Fire ants use their legs to link their bodies together into structural networks (Fig. 1A). These networks can be both temporary or long-lasting, such as rafts, bridges and bivouacs. Such devices must be able to survive perturbations by the elements, including raindrops or rough water currents. How ant-built structures sense damage and repair themselves is poorly understood.

The combination of individual efforts towards one goal is an age-old problem. This problem was formally discovered in 1913 by agricultural engineer Maximilien Ringelmann, who studied the effectiveness of farm animals used for pulling ploughs. He states that *When employing men, or draught animals, better use is achieved when the source of motive power works alone: as soon as one couples two or several such sources to the same load, the work performed by each of them, at the same level of fatigue, decreases as a result of the lack of simultaneity of their efforts.* Ringelmann verified his principle by observing humans in a tug of war. The result, later called the Ringelmann effect or social loafing, is striking: the contribution per individual decreases as much as 50% for a group of 8 compared to a single person. The phenomenon is not just restricted to a tug of war, but also appears in groups of individuals shouting or clapping.<sup>6</sup> Qualitative explanations for the phenomenon include lack of motivation, coordination between individuals, and individuals believing that their contribution does not matter inside a big group. Although Ringelmann effect has been shown using humans, it is unknown whether swarms of animals also exhibit it.

<sup>a</sup> School of Mechanical Engineering, Georgia Institute of Technology, Atlanta, GA 30332, USA. E-mail: [hu@me.gatech.edu](mailto:hu@me.gatech.edu)

<sup>b</sup> School of Physics and Astronomy, Rochester Institute of Technology, Rochester, NY 14623, USA

<sup>c</sup> School of Biology, Georgia Institute of Technology, Atlanta, GA 30332, USA

† Electronic supplementary information (ESI) available. See DOI: 10.1039/c6sm00063k

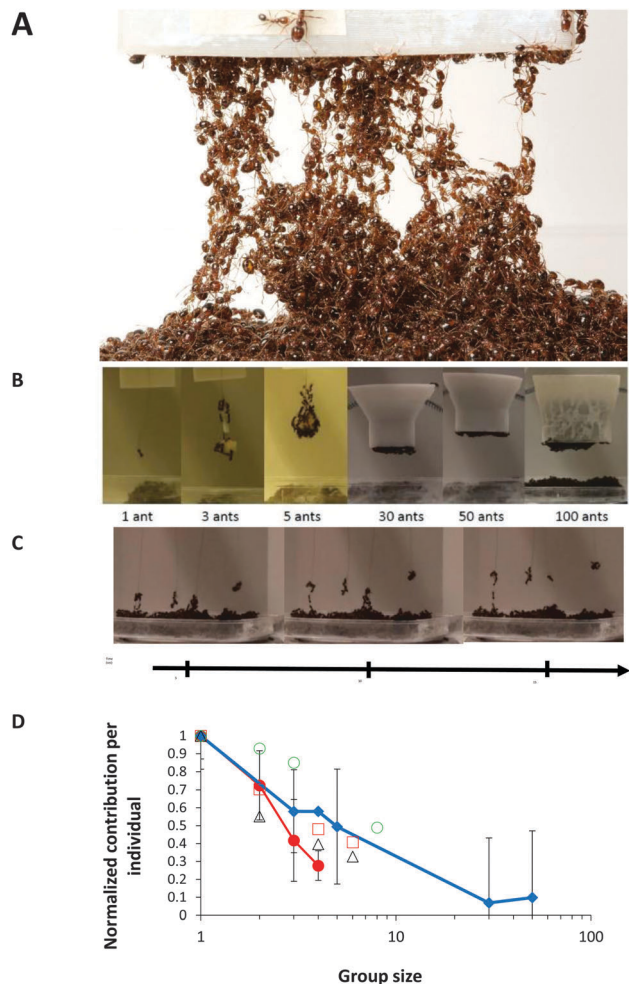


**Fig. 1** Tensile forces applied to ant aggregations. (A) Formation of strings and a mesh network due to the separation of an ant aggregation pressed together for 3 minutes. Photo credit – Candler Hobbs. (B) Testing rigs to measure the strength of groups of ants. (C) A tensile test of 4 isolated ants, each attached to a human hair. The hairs are pulled simultaneously. (D) Experiments showing Ringelmann effect in various organisms. The blue curve represents ants connected in an aggregation. The red curve represents isolated ants held by human hairs. The open symbols include a tug of war, clapping and shouting (circles, squares and triangles, respectively). Individual contribution is normalized with respect to tests with a single individual.

The cooperation of groups of living systems exhibit similarities with nonliving systems. Clusters of ants bear similarity to geometrically cohesive granular materials, which entangle due to the individual particle shape. These granular systems include long, thin rods in two-<sup>7</sup> and three-dimensions,<sup>8,9</sup> and U-shaped staples, which resist vibration<sup>10</sup> and extension.<sup>11</sup> In the case of rods, the cohesive forces required to resist pile breakup are generated purely from the lack of rotational freedom and friction. Stability is significantly greater in U-shaped particles, as the concave shape creates a significant entanglement density which governs rigidity.<sup>10</sup>

In this study, we show that fire ants compensate for Ringelmann effect by self-healing. We first present qualitative observations of ant connections. We then present experiments to measure

the adhesive strength of groups of ants. We rationalize our results using mathematical modeling and agent-based simulation. Lastly, we discuss our results and provide directions for future work.

## 2 Results

### 2.1 Qualitative observations of ants

Ants connect together using the hooks and sticky pads located at the tips of their legs.<sup>12</sup> We tie elastic bands around the waists of ants and used the bands to gently pull the ants apart. Using high speed videography, we observe two types of connections. Fig. 2A and B shows a leg-to-leg connection. Fig. 2C shows a leg-to-body connection. We use elastic bands to measure the strength of these connections. Leg–leg connections can support a tensile force of  $F_{\max} = 195 \pm 7$  dynes. Leg–body tensile force is much weaker, at  $69 \pm 52$  dynes.

To visualize how ants respond to forces, we manually separate two ant clusters and film the result using a high speed camera. Initially, ants form a mesh network where ants appear to be oriented randomly. As the two clusters are separated, the network stretches out into multiple strings of ants. These strings take the ants, which are originally oriented randomly,

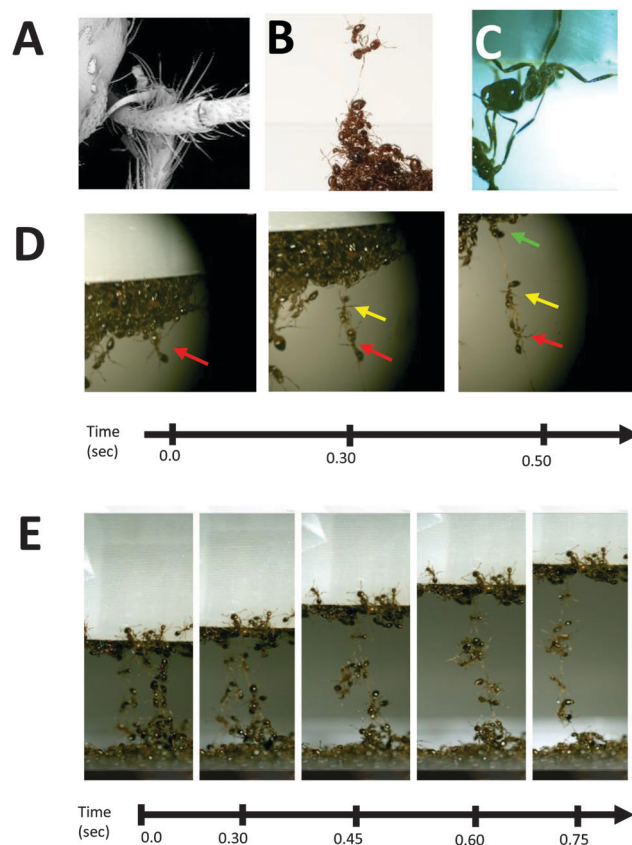


**Fig. 2** Cohesion of ants during tensile testing. (A) Close up of ants holding on to each other with tarsal claws. (B) Ants holding onto each other using sticky pads on their legs. (C) A close up view of an ant string being separated from a cluster. (D) Ants linking together using leg–leg connections. (E) Two ant strings combining during a tensile test.

and aligns them vertically. Fig. 2D shows the formation of an ant string. As the clusters are separated further, the string continues to lengthen as more ants are released from the cluster. Ant strings may also combine laterally to form longer strings. Fig. 2E shows two separate strings of ants that combine to become a single string. We notice that as the structures are stretched further, the connections slip, and leg-body connections transform into leg-leg connections.

## 2.2 Ringelmann effect in ants

We conduct tensile tests with groups of ants ranging from one to one hundred. This range exceeds that can be feasibly conducted with humans. Fig. 1A and B shows the testing rigs we 3-D printed to contain the ants for the measurement of tensile force. The cross-sectional area of the testing rig is proportional to the number of ants  $N$ , which is verified by counting the ants. Fig. 1D shows the relationship between group size and normalized contribution of each individual in the group. The group of  $N$  ants exerts a total force  $F_{\text{group}}$  in a tensile test. Each ant's individual contribution is  $F_{\text{group}}/N$ . The individual contribution is then divided by the maximum force  $F_{\text{max}}$  of a single ant, which we found earlier to be 195 dynes. Thus, the normalized contribution of a single ant is  $F_{\text{group}}/(NF_{\text{max}})$ . Similarly, the clapping data is found by measuring the acoustic intensity of a group, the number of members of the group, and the intensity of a single person clapping.<sup>6</sup> Normalization enables us to compare widely varying experiments, including humans in a tug of war, humans shouting and clapping shown by the open symbols (circles, squares, and triangles, respectively in Fig. 1D). These experiments show qualitative similarity to the ant experiments. The blue line shows the ant experiments. For groups of 30 ants, each ant provides only 15% of force provided by a single ant tugging by itself.

Ringelmann proposed that a lack of coordination was the cause of Ringelmann effect. To test this hypothesis, we conduct tensile tests with ants isolated from each other. We use individual testing rigs composed of 4 human hairs separated by 1 cm, as shown in Fig. 1C. Here the ants can only communicate to each other through the force they feel through the hair. In contrast, the previous test involved ants in direct contact with each other. Fig. 1D shows the contribution per ant for both isolated ants (red line) and ants in a group (blue line). The result shows that the Ringelmann effect exists in isolated ants as well. In fact, the effect is even stronger in isolated ants: in a group of 4 ants, each ant exerts 65% of the forces of non-isolated ants of a comparable group size. The discrepancy suggests that the lateral connections between ants help to strengthen the group.

## 2.3 Simulation

In this section, we compare experimental results to simulation. Fig. 3A shows the ants being pulled in tension and Fig. 3B shows how the simulated ants interact. We conduct a tensile test with 20 ants pulled apart at a speed of  $10 \text{ mm s}^{-1}$  or  $\sim 3$  ant body lengths per second (Fig. 4A). Fig. 4B shows a force–elongation relationship with the force data reported using a force sensor that provides finer time resolution. Due to the noise, we analyze the data using a 30 point running average. The force curve

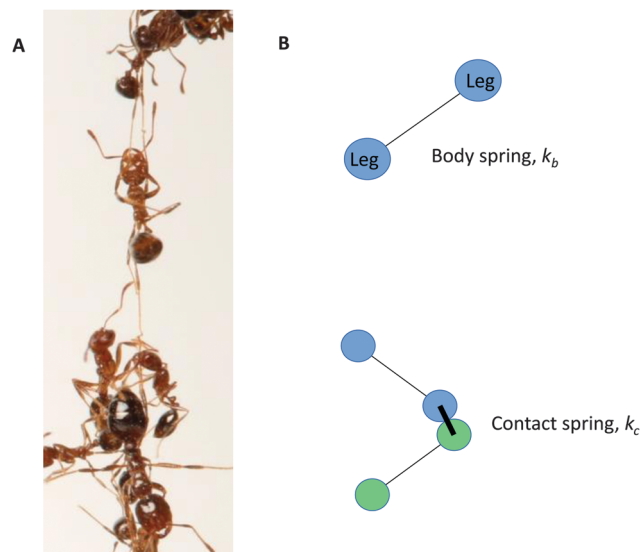
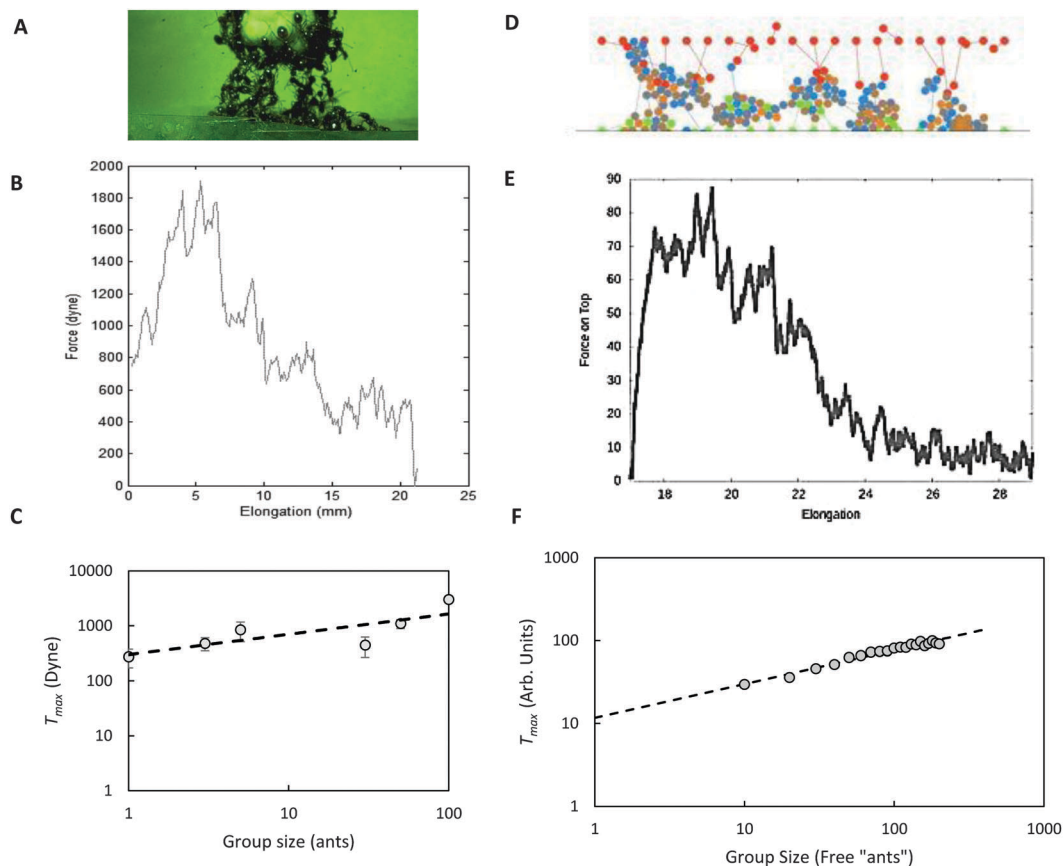


Fig. 3 Schematic of ants used in simulation. (A) Ants pulled in tension. (B) Simulated ants consist of two ants connected by a body spring of stiffness  $k_b$ . When ants make contact with a neighbor, they create a new Hookean contact with spring stiffness  $k_c$ .

shows many peaks throughout the entire test, which are likely due to rearrangements of the ant connections. These peaks are similar to those exhibited by tensile tests on the entangled pile of staples. Unlike staples, however, ants are active and are able to move their legs around to make new connections to rearrange.

We develop a Monte Carlo simulation that reproduces many of the behaviors seen in the ant-pile, most critically the fluctuating force as the pile is extended and the sub-linear scaling of maximum pile strength with size. The simulation is developed around the key idea that an ant that has its legs extended, stretched by its connection with neighbors, is less likely to let go than an ant with nearby neighbors. We posit that when an ant is stretched, it instinctively realizes that it plays an important role in keeping the pile coherent and is willing to withstand a greater force before letting go. We emphasize that this rule is at the level of individual ants.

In the simulation, the legs of an ant are modeled in pairs as small disks connected by an extensible massless body spring (length  $L$ , spring constant  $k_b$ ). Thus, ants in our simulation have only two feet, whereas actual ants have six feet. This body spring measures how much an individual ant is stretched. To account for the irregular movement of the ants, each disk is subjected to random forces, drawn from a uniform distribution between  $\pm F_{\text{mov}}$ , where  $F_{\text{mov}}$  represents the maximum movement force of an ant. As a result, the disks move about, loosely coupled to their partner “foot”. The disks interact through a Hookean repulsion with neighboring disks whose centers are closer than twice the disk radius, indicating contact. When contact is made with another disk, a second “contact” spring with much larger spring constant  $k_c \gg k_b$  is added to keep the disks in contact. These contact springs represent the tarsal claws of the ants. The relative value of the spring constants means that, as the disks continue to move at random and under the influence of



**Fig. 4** Ringelmann effect in experiments and simulations. Experiments are shown in (A–C), simulations in (D–F). (A) The ant tensile test. (B) Relationship between tensile force and elongation for a group size of 20 ants. To reduce the noise, we use a running average of 30 points. The fluctuations indicate the rearrangement of connections during the test. (C) The tensile strength, or maximum force, as a function of group size. The best fit line of power 0.37 is provided. (D) Simulated ants in a tensile test. Green ants are fixed to the bottom row, red ants are fixed to the top row which is moving upwards, and all other ants are colored to be distinguishable. Lines represent the body springs. (E) The relationship between force and elongation for 120 ants. (F) Maximum force of a tensile test as a function of the number of non-fixed ants. A best fit line of power 0.40 is provided.

other contacts, the disks in contact remain close to one another while the feet of an individual ant (connected by the body “spring”  $k_b$ ) can move apart and stretch. The following is a key rule in the simulation: the contact spring  $k_c$  breaks at random, representing the ants releasing their neighbor, but the probability decreases with the length of the body spring. This rule states that ants hold on tighter the more they are stretched. The contact spring also breaks if the tensile force exceeds a critical value. This second rule is analogous to the maximum force that we measured in ants connected by leg–leg connections. The disks move under Newtonian equations of motion, numerically evaluated with an Euler–Cromer integration.

To mirror experimental boundary conditions, a row of disk pairs (each pair representing the ant’s feet) are created with one disk fixed at the bottom and evenly separated horizontally. A similar row has one disk each fixed at the top. These boundary conditions represent ants that have half their bodies attached to the testing reg, and half their bodies within the aggregation. The remaining disk pairs, each representing one ant, are placed randomly within the space between the two fixed rows. The body springs are initially at an equilibrium length, with fluctuations occurring due to the random forces applied to the disks. The top row of fixed disks is then subjected to a

constant upward velocity; the net force required to maintain this motion is (by Newton’s third law) the force exerted on these disks by their connecting contact springs.

A snapshot of the simulation is shown in Fig. 4D. The fixed disks at the top are colored red; those fixed at the bottom are colored green. The connected network at this moment is heterogeneous, consisting of discrete chains involving only a few of the boundary disks. This heterogeneity is also seen in our ant experiments. The force required to steadily lift the top boundary fluctuates in time, as shown in Fig. 4E. In this figure, elongation units are given in terms of leg radius. Elongation represents the distance between the top and bottom row of fixed ants. Force is calculated as the sum of the forces applied by the top row body springs, in units of body spring constant times leg radius. The force initially increases almost linearly, corresponding to the time when the network is homogeneous and densely packed. Fluctuations correspond to significant rearrangements of the network, which becomes increasingly heterogeneous, and persist throughout the entire simulation. Similar experiments are seen in the experiment in Fig. 4B.

We conduct simulations with ant groups of varying size, from 10 to 500 ants. Ten independent simulations are run for each group size. The maximum force exerted by the group was

recorded and averaged over the ten runs. Fig. 4C and F show the maximum force of the group as a function of group size, for both the experiments and simulations. In the simulations, there are 20 ants each on the top and bottom. Maximum force represents the average of the maximum force over 10 runs. The experiments exhibit a power law fit with an exponent of 0.37; the simulations exhibit an exponent of 0.40, for group sizes less than 500 ants. Note that both exponents are less than one indicating that both experiments and simulation exhibit the Ringelmann effect.

## 2.4 Self-healing of ant aggregations

We press a pair of ant aggregations together for a given contact time  $\tau$ , ranging from 5 seconds to 15 minutes. We then conduct a tensile test, pulling them apart at constant velocity as shown by the schematic in Fig. 5A. The tensile test lasts for several seconds and is shown in the Video S1 (ESI<sup>†</sup>) and in time sequence in Fig. 5B. As stretching begins, tensile force increases. A peak in tensile force  $T_{\max}$  occurs, and then a decrease in force as the aggregations begin to neck and fracture. The relationship between force and strain during a test is shown in Fig. 5D, where each color corresponds to a different contact time. Since it is difficult to measure the cross-sectional area, we define the tensile strength in units of dynes rather than units of stress.

Qualitatively, ants pressed together for longer times appear to show a greater number of ant strings, which correspond to a higher tensile strength. Fig. 5C shows an increase in the number of ant strings with increasing contact time. We can measure this increasing strength quantitatively. Fig. 5E shows the relationship between tensile strength and contact time. The strength increases to a maximum of 3400 dyne at  $\tau = 8$  minutes. This measured strength is much less than the expected value if ants were pulling at maximum capacity. Given the cross-section of the aggregation as 100 ants, we would expect a strength of 21 000 dynes if ants were attached with leg–leg connections, and 7500 dyne if we assume all leg–body connections. Thus, ants are suffering a 50% loss of strength per ant due to the Ringelmann effect. The strength of the ant clusters also decreases with longer periods of time and because the ants have a natural tendency to explore, the cluster eventually breaks apart. This breaking is shown by the strength  $T_{\max}$  for  $\tau$  decreasing to 30% of its value as time elapses from 8 to 10 minutes.

## 2.5 Model of self-healing

We develop a model to explain this growth in strength,  $T$ , as a function of contact time,  $\tau$ . Once the ant aggregations are in contact, ants move their legs randomly until they connect with a member of the opposite aggregation. Let  $n(\tau)$  be the number of connections made between the aggregations, and  $N$  be the number of leg connections possible where  $N =$  two times the number of ants in a cross-section. We multiply by two because each ant has two legs that it can extend downward when it is held vertically. The number of connections made per minute,

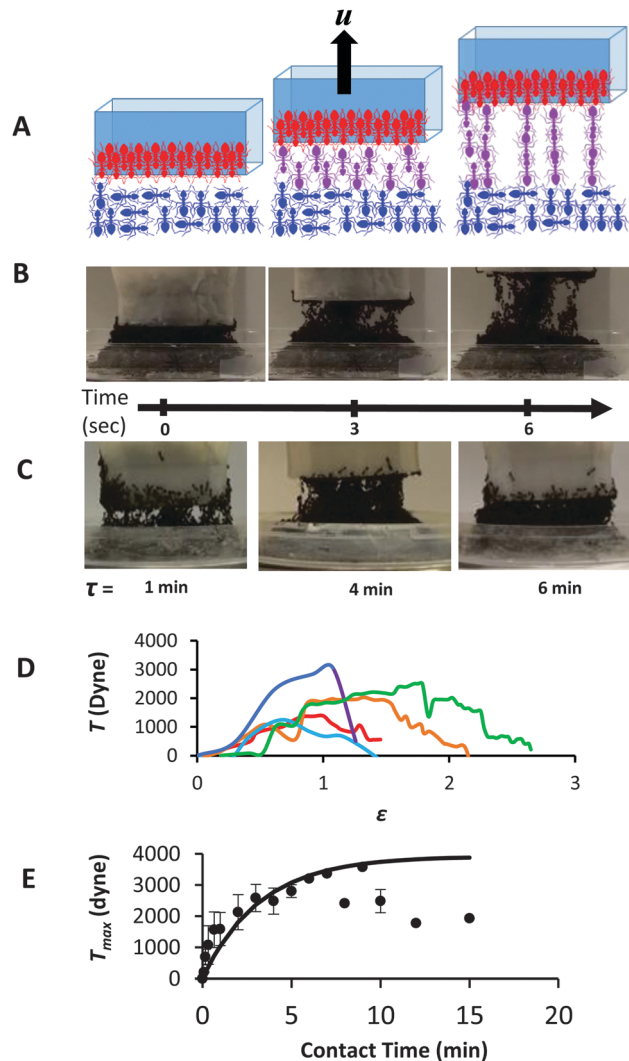


Fig. 5 Tensile strength of ant aggregations. (A) A schematic showing two ant clusters pulled apart. The top cluster is red and bottom cluster is blue. The purple ants are the connections that form between the clusters due to ants being extruded from the top and bottom layers. (B) Time sequence of the ant strings that form during the tensile test. (C) The tensile test can be conducted with different contact times that the clusters are pressed together. Shown is a time sequence of different contact times. Longer contact times create stronger connections, indicating self-healing of the clusters. (D) The relationship between tensile force and strain during a tensile test. The colors denote different contact times performed, 2 minutes (red), 4 minutes (orange), 5 minutes (green), 8 minutes (blue), and 10 minutes (purple). (E) The relationship between tensile strength  $T_{\max}$  and contact time.

$\frac{dn}{d\tau}$ , is proportional to  $N - n$ , the number of appendages that has not yet connected:

$$\frac{dn}{d\tau} = \beta(N - n) \quad (1)$$

where  $\beta$  is a constant with units of connections per minute. This differential equation explains the observations during experimentation. When we place two clusters in contact, initially there are no connections ( $n = 0$ ). At first, we find that

the rate at which ants are connecting is very rapid. As  $n$  increases to approach  $N$ , the rate plateaus. Solving the above differential equation yields the solution

$$n(\tau) = N(1 - \exp(-\beta\tau)), \quad (2)$$

where  $n(\tau)$  is the number of connection as a function of contact time  $\tau$ . Only connections that have been made can contribute to tensile strength of the aggregations. The associated tensile strength is found by multiplying by a constant  $\alpha$ , which has units of dynes per connections to get the strength as a function of contact time,

$$T_{\max}(\tau) = \alpha N(1 - \exp(-\beta\tau)). \quad (3)$$

Our model has two parameters,  $\alpha$  and  $\beta$ , that are found by curve-fitting, as well as an initial condition  $N$  given by the cross section of the ant aggregation. We use linear least squares to determine the tensile strength as a function of contact time. Fig. 5E shows that the prediction of the model closely matches the trends. The fitting parameters have a physical significance that we discuss in turn. We find that each connection yields a force of  $\alpha = 18.5$  dynes. This value is 10 times less than the leg-leg connection and 4 times less than leg-body connection measured from our experiment. We also learn of a rate constant by which self-healing occurs. The value  $\beta = 0.3$  connections per ant per minute indicates that every minute, 1 connection is made for every 3 available connections. In another way, consider 3 ant appendages waving around randomly; one in 3 makes a connection every minute.

We can use the model to predict how tensile force increases given the strain rate applied. We consider the number of ant strings available for lifting ants as a function of contact time. We consider each of these strings pulling out ants from the aggregation at a rate of  $u = 3.9 \text{ mm s}^{-1}$  or  $\dot{\epsilon} = u$  per ant length = 1.3 ant per second. Each of these ants lifted weighs  $m_{\text{ant}}$  where  $m_{\text{ant}} = 0.0015 \text{ g}$ , gravity  $g = 9800 \text{ mm s}^{-2}$ . Considering all  $n(\tau)$  chains, the weight of additional ants lifted per second is

$$\frac{dT}{dt} = \dot{\epsilon} m_{\text{ant}} g n(\tau). \quad (4)$$

Fig. 6A shows the time-rate of the change of tensile force  $\frac{dT}{dt}$  at  $t = 0$ , estimated as the average slope of the force during the first four seconds of the tensile test. The model is given by the black curve, which fits fairly against the data with a goodness of  $R^2$  of 0.48. Note that there are no free parameters in the prediction. All parameters are found from the previous fitting of  $T_{\max}$  and  $\tau$ . The fit suggests that the initial rate of increase in force is due to the increasing availability of ant strings.

Lastly, we show that the velocity chosen during our tensile tests does not strongly affect the outcome of the test. We place two clusters of ants together for  $\tau = 1$  minute and separate the cluster at velocities ranging from  $4 \text{ mm s}^{-1}$  to  $20 \text{ mm s}^{-1}$ . Fig. 6B shows that the tensile strength falls between a range of 14 000 to 25 000 dynes with no clear trends.

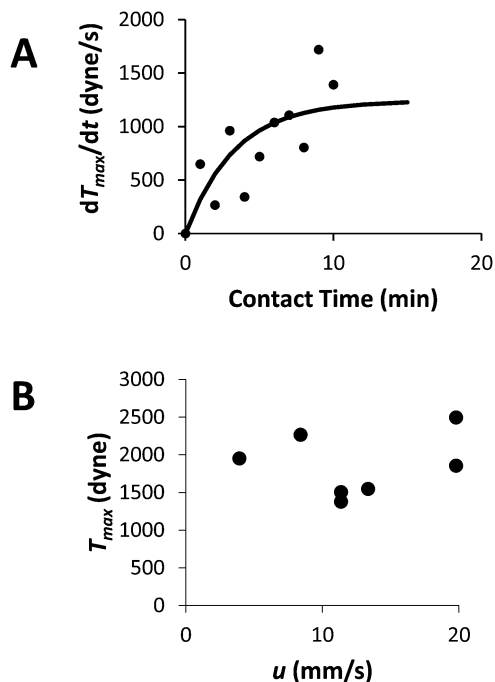


Fig. 6 (A) The relationship between contact time and the initial time-rate-of-change of tensile force. (B) The relationship between tensile strength and the speed of separation of the ant clusters.

### 3 Discussion

This study showed that fire ants succumb to the Ringelmann effect, with each ant contributing less to the total pile strength as the group size increased. In large groups, each ant contributed as little as 15% of its maximum strength. Simulations also showed this effect, with a sublinear scaling of pile strength  $T$  with group size  $g$  ( $T \propto g^{0.4}$ ). We note that the simulation has purely local interaction rules, with particle response governed solely by the immediate neighbors. This suggests that the origin of the Ringelmann effect (in this system) is purely statistical, a result of large-scale averaging over random variables, rather than the ants' awareness of the larger pile size. We also show, separately, that ants compensate for this effect by repairing their broken linkages over time.

In nature, growth and self-healing are often aspects of the same phenomenon. In this study, both processes are associated with the ants making new links with other ants, and changing the state of the structure. In a previous study,<sup>5</sup> we showed that a raft of 10 000 ants can rearrange itself from a sphere to a pancake within 2 minutes. This time scale is much shorter than the 10 minute time-scale of the group of 100 ants in the current study. The ability of ants to build connections may require light to illuminate the ant's surroundings. Ants on a raft only make connections on the surface of the raft. In our study, connections are made within the interface of two surfaces, where there is little light.

### 4 Conclusion

We use tensile testing to measure the strength of ant clusters as a function of group size and contact time. We find that each ant

contributes less to the group as the group size increases, a phenomenon known as the Ringelmann effect. To understand the causes for this phenomenon, we employ a two-dimensional simulation. This simulation relied on the following rule: ants randomly make and break connections, but grip each other with higher probability when stretched. The resulting simulation showed results similar to experiments. When two clusters are joined together, fire ants will self-heal into one connected structure. Using modeling, we found that the rate of connections made is proportional to the number of ants not yet connected. The rate at which new connections are made decreases with time, until saturation.

## 5 Materials and methods

### 5.1 Ant husbandry

We procured ant colonies from roadsides near Atlanta, GA. Colony selection aims for an average ant weight of 1.5 mg. We removed colonies from the soil and placed them into bins according to methods by Chen.<sup>13</sup> We fed ants baby food and pet food 3–4 times a week, along with constant replenishment of the water supply.

### 5.2 Micro-scale experiment

We measure the strength of leg–leg and leg–body connections to estimate the approximate load that the ants in an aggregate can carry. We measure the strength of the leg–leg connection by tying an ant to the elastic band and another ant of the same colony to an inelastic string. We place the two ants in contact to stimulate a leg–leg connection. Once the ants attach their legs, we pulled the inelastic string which causes the elastic band to stretch at a fixed distance. We then equate this distance to a force using Hooke's law. We also measure the leg–body connection using the same technique while stimulating a leg–body connection.

### 5.3 Tensile test

We place 4.0 grams of cluster on an analytical balance for all tensile tests and vary the top cluster. For the non-isolated tensile tests we put two ant aggregates in contact for contact times between 5 seconds to 15 minutes. For a group size of 1 ant, we tied 1 ant to a hair. For a group size of 3–5 ants, we attach ants to a sponge. For a group size of 30–100 we use 3D printed funnels that have enough space for 30–100 ants to go through. For isolated tensile tests we tie each ant on a single strand of hair, each separated by 1 cm. We varied the group size between 1 to 4 ants. All setups are attached to a motor that can produce testing speeds from 3.9 mm s<sup>-1</sup> to 20 mm s<sup>-1</sup>. The ant cluster on the bottom containing 4 grams is placed in a petri dish on top of a Metler Toledo analytical balance. We record the tests from the side view using a Sony HDR-XR200 handycam.

For the tensile test presented in Fig. 4, we put an ant pile of 5 grams on top of a petri dish lined with Velcro so that they

will grip. We then place a piece of Styrofoam of width 10 mm and depth 3 mm. The force is measured by using a Futek LS200 load sensor at a sampling frequency of 1 kHz and an Arduino Uno is used to measure the elongation length. All tests are performed at 10 mm s<sup>-1</sup>, unless stated otherwise.

## Acknowledgements

We thank J. L. Denouberg for suggesting the Ringelmann effect. This work was supported by the US Army Research Laboratory and the US Army Research Office Mechanical Sciences Division, Complex Dynamics and Systems Program, under contract number W911NF-12-R-0011.

## References

- 1 A. Rekondo, R. Martin, A. Ruiz de Luzuriaga, G. Cabanero, H. J. Grande and I. Odriozola, Catalyst-free room-temperature self-healing elastomers based on aromatic disulfide metathesis, *Mater. Horiz.*, 2014, **1**, 237–240.
- 2 G. J. Ackland, R. Hanes and M. H. Cohen, Self assembly of a model multicellular organism resembling the dictyostelium slime molds, 2007, arXiv:0705.0227, preprint.
- 3 J. A. Sherratt and J. D. Murray, Models of epidermal wound healing, *Proceedings of the Royal Societies of London*, 1990, **241**(1300), 29–36.
- 4 A. J. Singer and R. A. F. Clark, Cutaneous wound healing, *N. Engl. J. Med.*, 1999, **341**(10), 738–746, PMID: 10471461.
- 5 N. J. Mlot, C. A. Tovey and D. L. Hu, Fire ants self-assemble into waterproof rafts to survive floods, *Proc. Natl. Acad. Sci.*, 2011, **108**(19), 7669–7673, PMID: 10471461.
- 6 J. M. Levine and R. L. Moreland, *Small groups*, Psychology Press, 2006.
- 7 K. Stokely, A. Diacou and S. V. Franklin, Two-dimensional packing in prolate granular materials, *Phys. Rev. E: Stat., Nonlinear, Soft Matter Phys.*, 2003, **67**(5), 051302.
- 8 K. Desmond and S. V. Franklin, Jamming of three-dimensional prolate granular materials, *Phys. Rev. E: Stat., Nonlinear, Soft Matter Phys.*, 2006, **73**(3), 031306.
- 9 M. Trepanier and S. V. Franklin, Column collapse of granular rods, *Phys. Rev. E: Stat., Nonlinear, Soft Matter Phys.*, 2010, **82**, 011308.
- 10 N. Gravish, S. V. Franklin, D. L. Hu and D. I. Goldman, Entangled granular media, *Phys. Rev. Lett.*, 2012, **108**, 208001.
- 11 S. V. Franklin, Extensional rheology of entangled granular materials, *EPL*, 2014, **106**(5), 58004.
- 12 P. C. Foster, N. J. Mlot, A. Lin and D. L. Hu, Fire ants actively control spacing and orientation within self-assemblages, *J. Exp. Biol.*, 2014, **217**, 2089–2100.
- 13 J. Chen, Advancement on techniques for the separation and maintenance of the red imported fire ant colonies, *Insect Sci.*, 2007, **14**(1), 1–4.